

Comparative reactivity analysis of small-molecule thiol surrogates

László Petri, Péter Ábrányi-Balogh, Petra Regina Varga, Tímea Imre, György Miklós Keserű

PII: S0968-0896(20)30148-6  
DOI: <https://doi.org/10.1016/j.bmc.2020.115357>  
Reference: BMC 115357

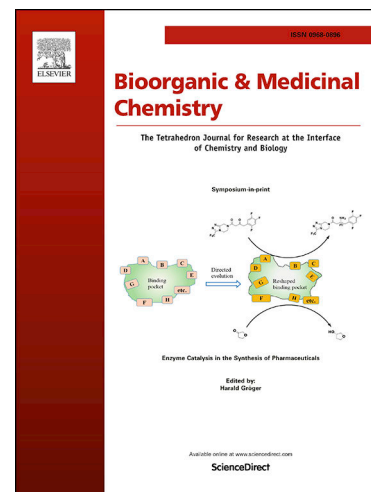
To appear in: *Bioorganic & Medicinal Chemistry*

Received Date: 11 November 2019  
Revised Date: 21 January 2020  
Accepted Date: 30 January 2020

Please cite this article as: L. Petri, P. Ábrányi-Balogh, P. Regina Varga, T. Imre, G. Miklós Keserű, Comparative reactivity analysis of small-molecule thiol surrogates, *Bioorganic & Medicinal Chemistry* (2020), doi: <https://doi.org/10.1016/j.bmc.2020.115357>

This is a PDF file of an article that has undergone enhancements after acceptance, such as the addition of a cover page and metadata, and formatting for readability, but it is not yet the definitive version of record. This version will undergo additional copyediting, typesetting and review before it is published in its final form, but we are providing this version to give early visibility of the article. Please note that, during the production process, errors may be discovered which could affect the content, and all legal disclaimers that apply to the journal pertain.

© 2020 Published by Elsevier Ltd.





## Comparative reactivity analysis of small-molecule thiol surrogates

László Petri<sup>a</sup>, Péter Ábrányi-Balogh<sup>a</sup>, Petra Regina Varga<sup>a</sup>, Tímea Imre<sup>b</sup> and György Miklós Keserű<sup>a,\*</sup><sup>a</sup>Research Centre for Natural Sciences, Medicinal Chemistry Research Group, H-1117, Budapest, Magyar tudósok krt 2, HU.<sup>b</sup>Research Centre for Natural Sciences, MS Metabolomics Research Group, H-1117, Budapest, Magyar tudósok krt 2, HU.

## ARTICLE INFO

## ABSTRACT

*Article history:*

Received

Received in revised form

Accepted

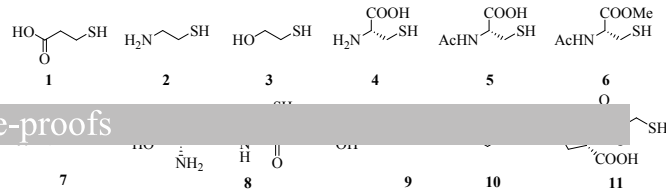
Available online

*Keywords:*cysteine reactivity  
covalent fragments  
thiol surrogate  
warhead  
cysteamine  
cysteine  
glutathione  
reactivity assay

Discovery of targeted covalent inhibitors' discovery is an increasingly popular approach to challenging drug targets. Since covalent and non-covalent interactions are both contributing to the affinity of these compounds, evaluation of their reactivity is a key-step to find feasible warheads. There are well-established HPLC- and NMR-based kinetic assays to tackle this task, however, they use a variety of cysteine-surrogates including, cysteamine, cysteine or acetyl-cysteine and GSH. The diverse nature of the thiol sources often makes the results incomparable that prevents compiling a comprehensive knowledge base for the design of covalent inhibitors. To evaluate kinetic measurements from different sources we performed a comparative analysis of the different thiol surrogates against a designed set of electrophilic fragments equipped with a range of warheads. Our study included seven different thiol models and 13 warheads resulting a reactivity matrix analysed thoroughly. We found that the reactivity profile might be significantly different for various thiol models. Comparing the different warheads, we concluded that – in addition to its human relevance - glutathione (GSH) provided the best estimate of reactivity with highest number of true positives identified.

2009 Elsevier Ltd. All rights reserved.

\* Corresponding author. Tel.: +36-1-382-6821; e-mail: [keseru.gyorgy@ttk.hu](mailto:keseru.gyorgy@ttk.hu)



## 1. II

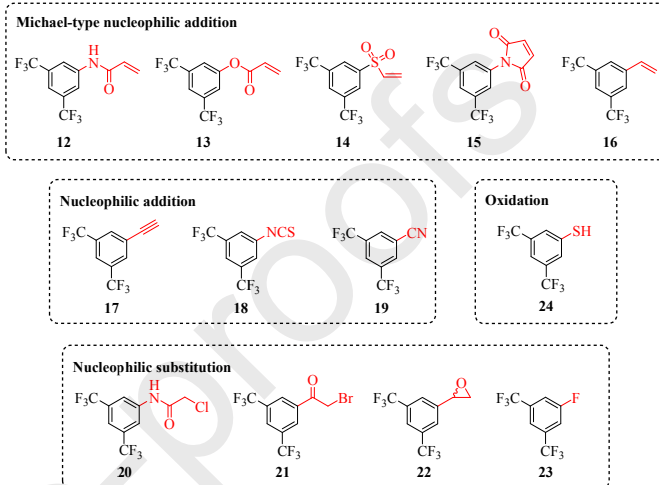
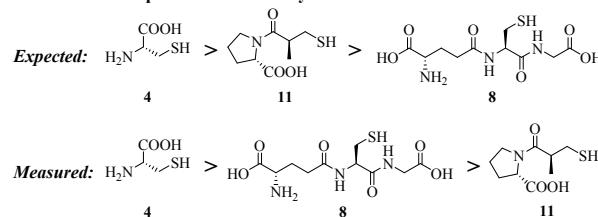
Compounds binding covalently to their protein targets have become increasingly popular in both chemical biology and drug discovery programs.<sup>1-3</sup> Exploiting the formation of a permanent covalent bond with an appropriate nucleophilic residue, these agents can be used for protein labelling, and in particular, targeting endogenous proteins considered as “undruggable”. Covalent binding might provide significant advantages such as the increased biochemical efficiency, high ligand efficiency and prolonged duration of action leading to less frequent dosing.<sup>2,4,5</sup> They could target shallow or featureless binding sites<sup>6-8</sup> and even intrinsically disordered proteins without definite binding sites. Target interactions of the covalent compounds first involves non-covalent contact. The formation of the non-covalent complex is followed by the reaction of the electrophilic functional group—usually called warhead—and the surrounding nucleophilic amino acid residue.<sup>9</sup> These residues include mostly cysteines, but lysines, tyrosines, threonines and serines could also be considered.<sup>10</sup> Although the non-covalent interactions are mainly responsible for the specificity of the compound, careful optimization of the warhead position and reactivity are also needed for the accurate covalent design.<sup>11-14</sup> This has been confirmed recently by proteomic studies indicating that cysteine reactivity might be remarkably diverse in distinct proteins.<sup>15</sup> Safety concerns about non-specific covalent binding<sup>16</sup> and the diverse reactivity of tractable cysteines created a substantial demand for surrogate thiol models for reactivity evaluations. There are numbers of studies applying HPLC- or NMR-based reactivity assays,<sup>17-23</sup> however, many of these are utilizing different small molecule cysteine surrogates. Thiol reactivity of electrophiles was estimated by the reaction with mercaptopropionate (**1**),<sup>24</sup> 2-aminoethanethiol (**2**, cysteamine),<sup>25</sup> 2-mercaptoethanol (**3**),<sup>26</sup> but amino acids, derivatives and peptides can be also used, as cysteine (**4**),<sup>27</sup> *N*-acetyl-cysteine (**5**),<sup>28</sup> *N*-acetyl-cysteine methyl ester (**6**),<sup>29</sup> *N*-*tert*-butyloxycarbonyl-cysteine methyl ester (**7**)<sup>23</sup> and glutathione (**8**, GSH).<sup>17</sup> Moreover, sulphur analogues of alcoholic and phenolic compounds are claimed to be useful as appropriate surrogates: alkyl-mercaptans (**9**)<sup>30</sup> or thiophenol (**10**)<sup>31</sup> (Figure 1a). Notably, out of these surrogates, cysteine (**4**) and GSH (**8**) are both present in serum. One of the most studied surrogate is obviously cysteine (**4**) that was the main subject of kinetic measurements since the 1930s. There are many studies investigating the thiol reactivity of cysteine (**4**), however, only few considered the reactivity of the thiol and the amino groups parallel.<sup>24</sup> The other most popular reactivity testing surrogate is using GSH (**8**) and have been implemented in ADMET screening and evaluating electrophiles reactivity such as haloacetic acids,<sup>32</sup> nitrophenyl- and benzyl halides,<sup>33</sup> iodoethyl alcohols,<sup>34</sup> acrylates and methacrylates<sup>35,36</sup>.

**Figure 1.** a) Small molecule cysteine-surrogates applied in reactivity assays. b) Theoretical (expected) and experimental (measured) reactivity order of thiol models determined by Bent *et al.*<sup>27</sup>

Investigating electrophiles against multiple thiol surrogates is a relatively rare approach. Acrylamide reactivity was evaluated experimentally and theoretically against three different nucleophilic partners including *L*-cysteine (**4**), *L*-glutathione (**8**) and captopyrl (**11**) (Figure 1b)<sup>27</sup> and a significant difference in reactivity was obtained. Notably, it has also been found that experimental and theoretical reactivity orders were different.

These results together with the increasing popularity of covalent approaches prompted us to investigate different reactivity models against a set of electrophiles. Here, we present the comparative analysis of seven thiol surrogates used for the reactivity evaluation of 13 covalent fragments equipped with different warheads. Our data might help selecting the most

## b) Theoretical and experimental reactivity order of thiol models



appropriate model for a particular warhead and furthermore, prioritizing the most predictive thiol surrogates in drug discovery screening cascades.

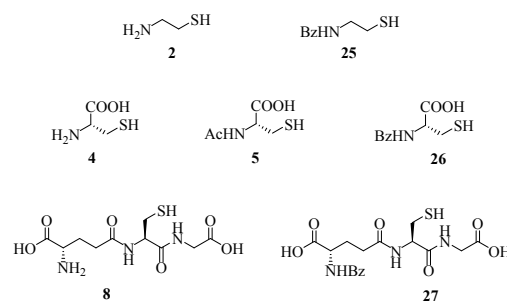
## 2. Results and discussion

## 2.1. Investigated covalent probes and thiol surrogates

For the comparative kinetic analysis, we applied a collection of covalent fragments (Figure 2) representing 13 different electrophilic warheads (**12-24**). Due to the different reactivity and binding mechanisms of these fragments, the measured reactivities cover a wide range of half-lives.

**Figure 2.** The electrophilic fragments (**12-23**) used as reactivity probes.

In order to investigate the reactivity of the electrophilic functional groups in an unbiased way, the different warheads were equipped to the same 3,5-bis(trifluoromethyl)phenyl scaffold. This core (**1**) provides robust signal in UV/VIS spectroscopy for the fragments, (**2**) it has no interference with any of the assay ingredients, (**3**) it forms no polar interactions, and (**4**) due to the electron-withdrawing character of the trifluoromethyl groups, it increases the reactivity at the electrophilic site. Notably, the CF<sub>3</sub> group is commonly used because of its chemical inertness and stability, that is related to the C-F bonds. The most abundant chemistry subtype was Michael-type conjugate nucleophilic addition (Ad<sub>NM</sub>), that is represented in 5 fragments (**12-16**). We included 3 fragments (**17-19**) reacting in nucleophilic additions (Ad<sub>N</sub>), 4 compounds (**20-23**) with nucleophilic substitution (S<sub>N</sub>) and one (**24**) with oxidation (Ox) mechanisms. The library was assembled by acquisition of the compounds or their intermediates either from commercial sources or by synthesis.



(cysteamine (**2**), *L*-cysteine (**4**) and *L*-glutathione (**8**) on Figure 3) were selected from the literature. We intended to investigate the *S*-nucleophilic reactivity independently of the *N*-nucleophilic site and therefore we prepared the corresponding *N*-protected derivatives. Thus, the surrogate set included *N*-acetyl cysteine (**5**) and the *N*-benzoylated derivatives of cysteamine (**25**), *L*-cysteine (**26**) and *L*-glutathione (**27**) (for the synthesis details see Experimental section). We used the benzoyl-group in order to improve detection by UV/VIS and also to provide better chromatographic separation for the thiol models and for their corresponding covalent adduct.

**Figure 3.** Small molecule cysteine-surrogates used in this study.

## 2.2. Reactivity assay

evaluated by the HPLC-based kinetic assay introduced by Flanagan *et al.*<sup>20</sup>. Additionally, we applied a correction based on the aqueous stability of the probes, as we described recently.<sup>17</sup> Reactions were conducted with a large excess of the thiols to ensure pseudo first order kinetics and linearity in the consumption of the electrophilic probes. Indoprofen was used as a stable and non-interfering internal standard in all HPLC measurements. Control experiments were performed without a thiol surrogate to characterize the aqueous stability of the probes. Relevant kinetic parameters were calculated from kinetic assay data as described recently by Ábrányi-Balogh *et al.*<sup>17</sup> Covalent adducts were analysed by HPLC-MS or HPLC-MS/MS measurements performed similarly to the kinetic assay but incubating at room temperature for 24 hours without the internal standard. One should note, that no solubility issues have been faced with, as no precipitation was observed during the experiments.

**Table 1.** Half-lives (h) measured for the electrophilic probes with different thiol models, corrected with the intrinsic aqueous stability of the compounds. Colour range is continuous from green to red where the dark green cells represent the hyper-reactive and dark red cells the unreactive probes against the corresponding surrogate.

Entry	Warhead chemotype	cysteamine 2	<i>N</i> -benzoyl- cysteamine 25	cysteine 4	<i>N</i> -acetyl- cysteine 5	<i>N</i> -benzoyl- cysteine 26	glutathione 8	<i>N</i> -benzoyl- glutathione 27
12	acrylamide	1.8	5.3	0.8	6.1	5.5	4.2	5.7
13	acrylate	<0.017*	<0.017*	<0.017*	<0.017*	<0.017*	<0.017*	<0.017*
14	vinylsulfone	<0.017*	<0.017*	<0.017*	<0.017*	<0.017*	<0.017*	<0.017*
15	maleimide	<0.017*	<0.017*	<0.017*	<0.017*	<0.017*	<0.017*	<0.017*
16	styrene	>50	>50	>50	>50	>50	>50	>50
17	acetylene	>50	2.4	>50	5.9	1.6	>50	0.3
18	isothiocyanate	<0.017*	<0.017*	<0.017*	<0.017*	<0.017*	<0.017*	<0.017*
19	nitrile	>50	>50	>50	>50	>50	>50	>50
20	chloroacetamide	4.4	0.8	3.6	5.4	5.5	5.8	>50
21	bromoacetophenone	<0.017*	<0.017*	<0.017*	<0.017*	<0.017*	<0.017*	<0.017*
22	epoxide	>50	>50	>50	>50	>50	6.0	>50
23	fluorobenzene	>50	>50	>50	>50	>50	11.0	>50
24	thiol	>50	>50	>50	33.0	>50	31.5	11.2

\* 0.017 h is the average lag-time between the zero-point measurement and manual mixing of the particular electrophilic probe and the investigated surrogate

## 2.3. Comparative analysis of thiol reactivity

The reactivity of the electrophilic probe library was investigated by an HPLC-based assay against 7 different small molecule cysteine surrogates. The kinetic dataset was used comparing different thiol models. Kinetic parameters, including the degradation kinetic constant ( $k_{deg}$ ), the measured kinetic constant ( $k_{app}$ ) and the effective reaction kinetic constants ( $k_{eff}$ ) and the derived half-life time are given in the Supplementary Material (Table S1). Here we focus only to measured half-lives (Table 1). Fragments with half-life time below 50 h were considered reactive.<sup>17,37</sup> Adduct formation was confirmed in dedicated HPLC-MS measurements (Supplementary Table S2). For the thiol surrogates with both *S*- and *N*-nucleophiles the adducts were investigated by HPLC-MS/MS and the reaction selectivity towards the *S*-nucleophile was confirmed in every case.

Horizontal analysis of the reactivity dataset (Table 1, rows) revealed that five probes (acrylate, **13**; vinylsulfone, **14**; maleimide, **15**; isothiocyanate, **18** and bromoacetophenone, **21**) reacted immediately with all the surrogates. As the average lag-

time between the zero-point measurement and manual mixing of the reaction was 1 min, and we did not observe any remaining traces of the fragment in the zero-point spectrum, we can conclude that half-lives in these cases is below the inevitable lag-time, numerically 0.017 h. On contrary, styrene (**16**) and nitrile (**19**) did not react with any of the thiols. The remaining electrophilic probes gave variable selectivity and sensitivity in the thiol assays. Epoxide (**22**), fluorobenzene (**23**) and thiol (**24**) showed considerable reactivity with one preferred thiol surrogate. Here we should note that epoxide (**22**) is a chiral molecule but we have applied that as a racemic mixture. Reacting with asymmetric thiols leads to diastereomeric products, but even in the only case when a reaction occurred, we did not observe duplicated peak belonging to the formed adduct. The epoxide (**22**) showed  $t_{1/2} = 6.0$  h and the fluorobenzene (**23**) showed  $t_{1/2} = 11.0$  h with glutathione (**8**), while the thiol (**24**) preferred *N*-benzoyl-glutathione (**27**), resulting in  $t_{1/2} = 11.2$  h. These preferences could be explained by structural or size attributions, steric or electronic features (such as the presence or absence of intra- or intermolecular H-bonds, surface accessibility of the active nucleophilic site, nucleophilicity of the

chemical studies. Notably, only GSH identified all of these fragments (**22**, **23**, **24**) as actives. Comparing the kinetic results obtained with free- and protected *N*-nucleophiles we found that in spite of its low reactivity against cysteamine (**2**), cysteine (**4**) or glutathione (**8**), the acetylene (**17**) showed higher reactivity with *N*-protected thiol surrogates (**5**, **25**, **26**, **27**). The acrylamide (**12**) reacted with all of the thiol models with reasonable half-lives that supports its most abundant application among covalent inhibitors. It was the most reactive against cysteine (**4**), resulting  $t_{1/2} = 0.8$  h, while the lowest reactivity ( $t_{1/2} = 6.1$  h) was observed with *N*-acetyl-cysteine (**5**). The chloroacetamide (**20**) probe was reacted quite similar, resulting in 4.4 h, 3.6 h and 5.8 h, respectively for cysteamine (**2**), cysteine (**4**) and glutathione (**8**). The reactivity measured with *N*-protected cysteine derivatives (**5**, **25**, **26**, **27**) showed a diverse profile, as the most reactive was *N*-benzoyl-cysteamine with  $t_{1/2} = 0.8$  h, while the less reactive was found to be the *N*-benzoyl-glutathione ( $t_{1/2} > 50$  h).

These trends are often difficult to understand as many molecular properties could influence the intrinsic reactivity. In some cases, we noted decreasing reactivity after *N*-acylation of the thiol surrogate, which could be easily interpreted as the *N*-nucleophilic site also could react with the individual warhead. However, LC-MS/MS measurements revealed that no *N*-labeling could take place with the thiol surrogates having available  $\text{NH}_2$ . Another influencing issue could be the molecular size which could drastically change diffusion behavior and sterical properties, either. Moreover, intramolecular H-bond between the SH and  $\text{NH}_2$  functionalities could decrease the nucleophilicity of the sulphur, in this case the *N*-acylation could intensify the reactivity via eliminating the intramolecular SH-masking. Furthermore, sterical hindrance arisen by the introduction of the benzoyl group could influence reactivity and an electronic effect on the nucleophilicity of the sulphur could also take place by an electron withdrawing adjacent cationic  $\text{NH}_3^+$  (**2**, **4**, **8**). For better understanding and further discussion mechanistic studies and quantum chemical investigations should be addressed to these phenomenomes.

Next, we compared the reactivity of different thiol surrogates (vertical analysis of Table 1, columns). First, we conclude that *N*-benzoylation resulted in significant improvement of chromatographic separation and UV/VIS visibility of the thiol model compounds. In particular, the cysteamine (**2**) assay resulted in 7 actives out of the 13 probes, which included all the 5 hyper-reactive fragments (acrylate, **13**; vinylsulfone, **14**; maleimide, **15**; isothiocyanate, **18** and bromoacetophenone, **21**). One further probe showed moderate reactivity ( $t_{1/2} = 34.8$  h for acrylamide **12**). *N*-benzoyl-cysteamine (**26**) showed similar reactivity profile as its unprotected pair, only the acetylene (**17**) showed significant increase in reactivity. For cysteine (**4**) we have found 7 fragments active that again includes the 5 hyper-reactive ones. Comparing *N*-acetyl-cysteine (**5**) and *N*-benzoyl-cysteine (**26**), the two models showed quite similar reactivity profile to that found for **4**, however, *N*-protection resulted in serious decrease of the measured reactivity of the acrylamide (**12**). The follow-up MS/MS study revealed that the amino group of **4** did not react with this probe, increased half-lives are associated to the decreased reactivity of the thiol. An opposite effect was found for the acetylene (**17**), where the reactivity increased significantly due to the protection of the concurrent *N*-nucleophile. *N*-acetyl-cysteine (**5**) identified 9 probes as actives, showing a wide reactivity window up to 50 h. We have found 5 covalent fragments considered as hyper-reactive and 4 fragments as unreactive. In the case of glutathione (**8**) we have found the highest number of actives (10 out of the 13), which suggest this surrogate being highly specific and sensitive. One might notice that the acetylene (**17**) showed high reactivity against

against all of the unprotected surrogates (over 50 h).

Comparing the investigated thiol surrogates, we finally analysed the number of the positive hits and the explored reactivity window of the probe library. Hyper-reactive and unreactive probes were excluded here to evaluate only the fragments having measurable reactivity. Figure 4 shows the result of this analysis; number of the fragments are proportional with the size of the plots, while their distribution is depicted in reactivity bins covering the full reactivity range between 0 h and 50 h (0-5 h, 5-10 h, 10-20 h and 20-50 h). We have found that the most active probes were found in the glutathione (**8**) assay that covered the widest reactivity range. Our results reinforced that thiol reactivity is heavily dependent on the surrogate model used and suggest GSH (**8**) as the best option for screening covalent libraries.

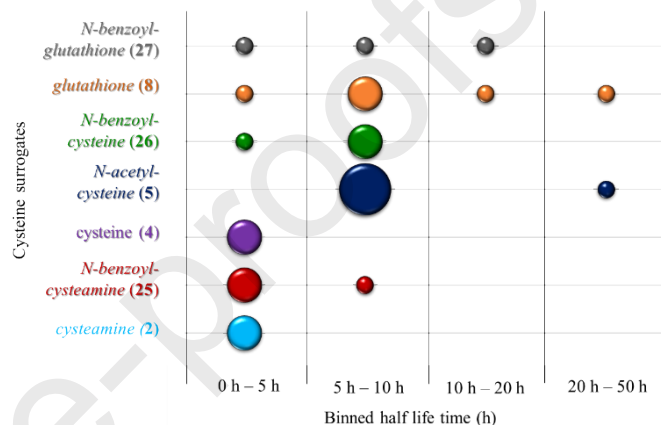


**Figure 4.** The distribution of half-lives in binned reactivity intervals. The results are separated by thiol models and the size of the plots are proportionate to the number of the fragments within the labelled reactivity window.

### 3. Conclusion

Here we investigated an electrophilic probe library against different thiol surrogates. Using an HPLC-based kinetic assay we measured the reactivity matrix including the pairwise reactivity of the investigated probe and model molecules. Based on the kinetic results we compared the thiol surrogates, to show up their scope and limitations in cysteine reactivity profiling. We made two important conclusions: (a) the different thiol surrogates results in different reactivity profile and (b) the glutathione (**8**) assay provided the best sensitivity and reactivity coverage for the electrophilic probe library profiled. These results demonstrate that the type of the thiol model has a high impact on the screening of electrophilic libraries. It could be concluded that the GSH assay might be suggested mostly to generate comparable and high-quality reactivity datasets for covalent compounds. In addition, it was also confirmed by LC-MS/MS that the GSH reacts with the investigated fragments only on its S-nucleophilic site.

### 4. Experimental

#### 4.1. Instruments

$^1\text{H}$  NMR spectra were recorded in  $\text{DMSO}-d_6$  or  $\text{CDCl}_3$  solution at room temperature, on a Varian Unity Inova 500 spectrometer (500 MHz for  $^1\text{H}$  NMR spectra), with the deuterium signal of the solvent as the lock and TMS as the internal standard. Chemical shifts ( $\delta$ ) and coupling constants ( $J$ ) are given in ppm and Hz, respectively.

HPLC-MS measurements were performed using a Shimadzu LCMS-2020 device equipped with a Reprospher 100 C18 ( $5\ \mu\text{m}$ ;  $100\times 3\text{mm}$ ) column and positive-negative double ion source

(DU m/z. Sample was eluted with gradient elution using eluent A (10 mM ammonium formate in water:acetonitrile 19:1) and eluent B (10 mM ammonium formate in water:acetonitrile 1:4). Flow rate was set to 1 ml/min. The initial condition was 0% B eluent, followed by a linear gradient to 100% B eluent by 1 min, from 1 to 3.5 min 100% B eluent was retained; and from 3.5 to 4.5 min back to initial condition with 5% B eluent and retained to 5 min. The column temperature was kept at room temperature and the injection volume was 10  $\mu$ l. Purity of compounds was assessed by HPLC with UV detection at 215 nm; all tested compounds were >95% pure. HPLC measurements were carried out with the same instrument without the mass spectrometry detector.

A Sciex 6500 QTRAP triple quadrupole – linear ion trap mass spectrometer, equipped with a Turbo V Source in electrospray mode (Sciex, CA, USA) and a Perkin Elmer Series 200 micro LC system (Massachusetts, USA) consisting of binary pump and an autosampler was used for LC–MS/MS analysis. Data acquisition and processing were performed using Analyst software version 1.6.2 (AB Sciex Instruments, CA, USA). Chromatographic separation was achieved by Purospher STAR RP-18 endcapped (50 mm  $\times$  2,1mm, 3 $\mu$ m) LiChocart® 55-2 HPLC Cartridge. Sample was eluted with gradient elution using solvent A (0.1% formic acid in water) and solvent B (0.1% formic acid in acetonitrile). Flow rate was set to 0.5 ml/min. The initial condition was 5% B for 2 min, followed by a linear gradient to 95% B by 6 min, from 6 to 8 min 95% B was retained; and from 8 to 8.5 min back to initial condition with 5% eluent B and retained to 14.5 min. The column temperature was kept at room temperature and the injection volume was 10  $\mu$ l. Nitrogen was used as the nebulizer gas (GS1), heater gas (GS2), and curtain gas with the optimum values set at 35, 45 and 45 (arbitrary units), respectively. The source temperature was 450 °C and the ion spray voltage set at 5000 V. Declustering potential value was set to 150V.

#### 4.2. Thiol reactivity assay<sup>17</sup>

For thiol reactivity assay 500  $\mu$ M solution of the fragment (PBS buffer pH 7.4, 10 % acetonitrile, 250  $\mu$ L) with 200  $\mu$ M solution of indoprofen as internal standard was added to 10 mM thiol model compound solution (dissolved in PBS buffer, 250  $\mu$ L) in 1:1 ratio. The final concentration was 250  $\mu$ M fragment, 100  $\mu$ M indoprofen, 5 mM thiol surrogate and 5 % acetonitrile (500  $\mu$ L). The final mixture was analyzed by HPLC after 0, 1, 2, 4, 8, 12, 24, 48, 72 h time intervals. Degradation kinetics was also investigated respectively using the previously described method, applying pure PBS buffer instead of the thiol model compound solution. In this experiment the final concentration of the mixture was 250  $\mu$ M fragment, 100  $\mu$ M indoprofen and 5 % acetonitrile. The AUC (area under the curve) values were determined via integration of HPLC spectra then corrected with internal standard. The fragments AUC values were applied for ordinary least squares (OLS) linear regression and for computing the important parameters (kinetic rate constant, half-life time) a programmed excel (Visual Basic for Applications) was utilized. The data are expressed as means of duplicate determinations, and the standard deviations were within 10% of the given values.

The calculation of the kinetic rate constant for the degradation and corrected thiol-reactivity is the following. Reaction half-life for pseudo-first order reactions is  $t_{1/2} = \ln 2/k$ , where  $k$  is the reaction rate. In the case of competing reactions (reaction with thiol surrogate and degradation), the effective rate for the consumption of the starting compound is  $k_{app} = k_{deg} + k_{eff}$ . When measuring half-lives experimentally, the  $t_{1/2(app)} = \ln 2/(k_{app}) = \ln 2/(k_{deg} + k_{eff})$ . In our case, the corrected  $k_{deg}$  and  $k_{app}$  (regarding to blank and GSH containing samples,

the datapoints of the kinetic measurements. The corrected  $k_{eff}$  is calculated by  $k_{app} - k_{deg}$ , and finally half-life time is determined using the equation  $t_{1/2(eff)} = \ln 2/k_{eff}$ .

Adducts were analysed by performing the same sample preparing protocol, then incubating the mixtures overnight at room temperature. Then LC-MS (for thiol models: 5, 26, 27, 28) or LC-MS/MS (for thiol models: 2, 4, 7) measurements were accomplished to determine the presence of the potential adduct.

#### 4.3. Synthesis

##### 4.3.1. *N*-(3,5-Bis(trifluoromethyl)phenyl)acrylamide (**12**)<sup>38</sup>

To a solution of 3,5-bis(trifluoromethyl)aniline (1.56 mL, 10 mmol) in dichloromethane (30 mL) triethyl amine (1.40 mL, 10 mmol) was added, and the mixture was allowed to stir under *Ar* at room temperature for 10 min. The mixture was cooled with iced water and then acryloyl chloride (0.81 mL, 10 mmol) was added dropwise, and the reaction was left to stir at room temperature for 2 h. The reaction was concentrated under vacuum. The residue was diluted with water and extracted with ethyl acetate. The organic layer was washed with 1 M aqueous solution of hydrochloric acid, dried over anhydrous sodium sulfate, filtered, and concentrated under vacuum. The product was washed with ether and then vacuum dried to afford **7** as a white powder (2.06 g, 70%). <sup>1</sup>H NMR (500 MHz, DMSO-*d*<sub>6</sub>):  $\delta$  10.76 (s, 1H), 8.32 (s, 2H), 7.76 (s, 1H), 6.37 (qd,  $J = 17.0$ , 5.9 Hz, 2H) 5.86 (dd,  $J = 9.7$ , 2.1 Hz, 1H) ppm.

##### 4.3.2. 3,5-Bis(trifluoromethyl)phenyl acrylate (**13**)

In 10 mL dichloromethane 3,5-bis(trifluoromethyl)phenol (0.15 mL, 1 mmol) and *N,N*-diisopropylethylamine (0.17 mL, 1 mmol) was dissolved and stirred at room temperature for 10 min. The reaction mixture was cooled with iced water and then acryloyl chloride (0.08 mL, 1 mmol) was added dropwise. Then the reaction was allowed to stir at RT overnight. The solvent was removed under vacuum and the residue was dissolved in ethyl acetate. The solution was washed with saturated sodium bicarbonate and water. The organic phase was dried over anhydrous sodium sulfate, filtered, and concentrated under vacuum. The product was purified by flash column chromatography using a mixture of hexane and ethyl acetate as eluent. The compound **8** was obtained as a colourless oil (39 mg, 14%) <sup>1</sup>H NMR (300 MHz, CDCl<sub>3</sub>):  $\delta$  7.82 (s, 1H), 7.70 (s, 2H), 6.72 (d,  $J = 17.2$  Hz, 1H), 6.39 (dd,  $J = 17.2$ , 10.5 Hz, 1H), 6.16 (d,  $J = 10.4$  Hz, 1H) ppm. <sup>13</sup>C NMR (75 MHz, CDCl<sub>3</sub>):  $\delta$  163.75, 151.33, 134.47, 133.21 (q,  $J = 34.1$  Hz, 2C), 127.12, 123.01 (d,  $J = 272.9$  Hz, 2C), 122.71 (2C), 120.49 – 119.43 (m) ppm. Anal. calcd. for C<sub>11</sub>H<sub>6</sub>F<sub>6</sub>O<sub>2</sub>: C, 46.47; H, 2.11. found: C, 46.38; H, 2.15.

##### 4.3.3. 3,5-Bis(trifluoromethyl)vinylsulfone (**14**)<sup>39</sup>

3,5-Bis(trifluoromethyl)thiophenol (505  $\mu$ L, 3 mmol) and potassium-carbonate (830 mg, 6 mmol) was dissolved in 25 mL *N,N*-dimethylformamide, then 2-chloroethanol (270  $\mu$ L, 4 mmol) was added and the mixture was stirred at room temperature. After 4 hours, the solvent was evaporated and the residue was dissolved in 50 mL ethyl acetate, then washed with 50 mL brine. The organic layer was dried and concentrated. The crude product was dissolved in 30 mL dichloromethane and meta-chloroperoxybenzoic acid (1.29 g, 7.5 mmol) was added slowly. The mixture was stirred for 3 hours, then it was washed with 1M aqueous solution of sodium hydroxide. After the extraction the organic phase was dried and concentrated, then the product was dissolved in 20 mL dry dichloromethane. To this solution methanesulfonyl-chloride (230  $\mu$ l, 3 mmol) was added at 0 °C, then triethylamine (625  $\mu$ L, 4.5 mmol) was dropped slowly into the mixture. After the addition of the base, the reaction was heated up to room temperature and

stirr

product was purified by column chromatography to give the **14** vinyl-sulfone product (128 mg, 14%) <sup>1</sup>H NMR (500 MHz, DMSO-*d*<sub>6</sub>): δ 8.34 (s, 2H), 8.13 (s, 1H), 6.74 – 6.61 (m, 2H), 6.24 (d, J = 8.7 Hz, 1H) ppm.

#### 4.3.4. 1-(3,5-Bis(trifluoromethyl)phenyl)-1H-pyrrole-2,5-dione (**15**)<sup>40</sup>

To a solution of maleic anhydride (214 mg, 2.18 mmol) in dichloromethane (20 mL) 3,5-bis(trifluoromethyl)aniline (0.34 mL, 2.2 mmol) was added dropwise at 40 °C, and the mixture was allowed to stir for 2 h. The intermediate was obtained as white crystals (705 mg, 98 %) and collected by filtration. The intermediate was dissolved in toluene (30 mL), then catalytic sulfuric acid was added (1-2 drops). The reaction flask was equipped with a Dean-Stark apparatus and the mixture was refluxed at 130 °C for 3 h. The solvent was removed under vacuum and the residue was purified by flash column chromatography with a mixture of hexane and ethyl acetate as eluent. The product was obtained as brown solid (272 mg, 40 %). <sup>1</sup>H NMR (500 MHz, DMSO-*d*<sub>6</sub>): δ 8.15 (s, 1H), 8.12 (s, 2H), 7.27 (s, 2H) ppm.

#### 4.3.5. N-(3,5-Bis-trifluoromethyl-phenyl)-2-chloro-acetamide (**20**)<sup>41</sup>

The same procedure as for **12** except using chloroacetyl chloride (0.80 mL, 10 mmol). Pure **21** was obtained as a white powder (2.31 g, 75%). <sup>1</sup>H NMR (500 MHz, DMSO-*d*<sub>6</sub>): δ 10.90 (s, 1H), 8.24 (s, 2H), 7.80 (s, 1H), 4.32 (s, 2H) ppm.

#### 4.3.6. 1-(3,5-Bis(trifluoromethyl)phenyl)-2-bromoethanone (**21**)<sup>42</sup>

To a stirred solution of 0.18 mL 3',5'-bis(trifluoromethyl)acetophenone (1 mmol) in 10 mL tetrahydrofuran 0.32 pyridinium-tribromide (1 mmol) was added dropwise in 10 mL tetrahydrofuran. The reaction mixture was stirred for 4 h. Water (20 mL) was added, and the mixture was separated. The aqueous phase was extracted with 2 x 20 mL ethyl acetate. The organic phase was dried over magnesium sulfate, and evaporated to silica. Flash column chromatography using hexane – ethyl acetate 95:5 as the eluent afforded the **22** product (190 mg, 57%) as a yellow oil that solidified overnight. <sup>1</sup>H NMR (500 MHz, DMSO-*d*<sub>6</sub>): δ 8.55 (s, 2H), 8.44 (s, 1H), 5.12 (s, 2H) ppm.

#### 4.3.7. 2-(3,5-Bis(trifluoromethyl)phenyl)oxirane (**22**)<sup>43</sup>

3,5-Bis(trifluoromethyl)phenyl-styrene (0.36 mL, 2 mmol) was dissolved in 20 mL chloroform, and 1.38 g 3-chloroperbenzoic acid (4 mmol) was added at 0 °C. The reaction mixture was stirred overnight, followed by washing with 10 mL saturated aqueous solution of sodium bicarbonate. The organic phase was dried over magnesium sulfate and evaporated to silica. The crude product was purified with flash chromatography using hexane – ethyl acetate 93:7 as the eluent. <sup>1</sup>H NMR (500 MHz, CDCl<sub>3</sub>): δ 7.82 (s, 1H), 7.74 (s, 2H), 3.99 (dd, J = 3.8, 2.6 Hz, 1H), 3.23 (dd, J = 5.3, 4.1 Hz, 1H), 2.79 (dd, J = 5.4, 2.4 Hz, 1H) ppm.

#### 4.3.8. N-(2-mercaptoethyl)benzamide (**25**)<sup>44</sup>

Cysteamine hydrochloride (341 mg, 3 mmol) was dissolved in 15 mL dichloromethane and benzoyl-chloride (280 μL, 3 mmol) and triethylamine (835 μL, 6 mmol) was added at 0 °C, under *Ar* atmosphere. After addition the reaction mixture was stirred at room temperature overnight. The reaction was extracted with 25 mL saturated aqueous solution of sodium bicarbonate, then the aqueous layer was washed with 2x15 mL dichloromethane. The organic layer was dried and concentrated, then purified by reversed phase column chromatography applying acetonitrile : water gradient elution. The **26** product was obtained as white solid (203 mg, 37%). <sup>1</sup>H NMR (500 MHz, DMSO-*d*<sub>6</sub>): δ 7.72 (d, J = 7.2 Hz, 2H), 7.45 (t, J = 7.4 Hz, 1H), 7.38 (t, J = 7.5 Hz, 2H), 6.56 (s,

(t, J = 8.5 Hz, 1H) ppm.

#### 4.3.9. 2-benzamido-3-mercaptopropanoic acid (N-benzoyl-cysteine) (**26**)

Reduced *L*-cysteine (0.5 g; 4.13 mmol) was dissolved in 10 mL *N,N*-dimethylformamide, and 575 μL triethylamine was added (4.13 mmol). The reaction mixture was cooled on ice and half-equivalent of benzoyl-chloride (240 μL, 2.06 mmol) was added dropwise, the the mixture was stirred overnight. Then the solvent was removed under reduced pressure, then the residue was dissolved in 15 mL brine and washed with 3x15 mL ethyl acetate. The organic phase was dried, filtered and evaporated. Then the crude product was purified on reversed phase column chromatography, applying acetonitrile-water gradient to yield 211 mg (46%) of **26** product. <sup>1</sup>H NMR (500 MHz, CDCl<sub>3</sub>): δ 11.06 (s, 1H), 7.87 (d, J = 7.2 Hz, 2H), 7.55 (t, J = 7.4 Hz), 7.48 (t, J = 7.5 Hz, 2H), 7.14 (d, J = 5.4 Hz, 1H), 5.07 – 5.03 (m, 1H), 3.23 – 3.19 (m, 2H), 1.50 (t, J = 9.0 Hz, 1H) ppm.

#### 4.3.10. 2-benzamido-5-((1-((carboxymethyl)amino)-3-mercaptopropan-2-yl)amino)-5-oxopentanoic acid (N-benzoyl-glutathione) (**27**)

First oxidized *L*-glutathione (1000 mg, 1.63 mmol) was acylated with benzoyl-chlorid (378 μL, 3.26 mmol) in *N,N*-dimethylformamide, in the presence of triethylamine (453 μL, 3.26 mmol). After, the reaction was completed, the solvent was removed under reduced pressure, then the residue was dissolved in 50 mL ethyl acetate and washed with 50 mL brine. The organic phase was dried, filtered and evaporated. Then the crude product was dissolved in 30 mL water : tetrahydrofuran 1 : 100 solvent mixture, then triphenylphosphine (427 mg, 1.63 mmol) was added and the reaction mixture was stirred at 50 °C overnight. After the reduction was completed the solvent was evaporated and the residue was directly purified by reversed phase column chromatography, applying acetonitrile-water gradient elution to give the **27** product (160 mg, 24%). <sup>1</sup>H NMR (500 MHz, CDCl<sub>3</sub>): δ 7.87 (d, J = 7.3 Hz, 2H), 7.56 – 7.49 (m, 1H), 7.49 – 7.42 (m, 2H), 4.46 – 4.26 (m, 2H), 3.77 – 3.64 (m, 2H), 2.88 – 2.71 (m, 1H), 2.71 – 2.55 (m, 1H), 2.37 – 2.21 (m, 2H), 2.12 – 2.08 (m, 1H), 1.99 – 1.93 (m, 1H) ppm.

### Declaration of Competing Interest

The authors declare that they have no conflict of interest.

### Acknowledgements

Financial support of H2020 MSCA FRAGNET (project 675899), National Research Development and Innovation Office (grant number SNN\_17 125496) and by the Slovenian Research Agency (grant number N1-0068 (B) and research core funding No. P1-0208) and OTKA PD124598 is gratefully acknowledged.

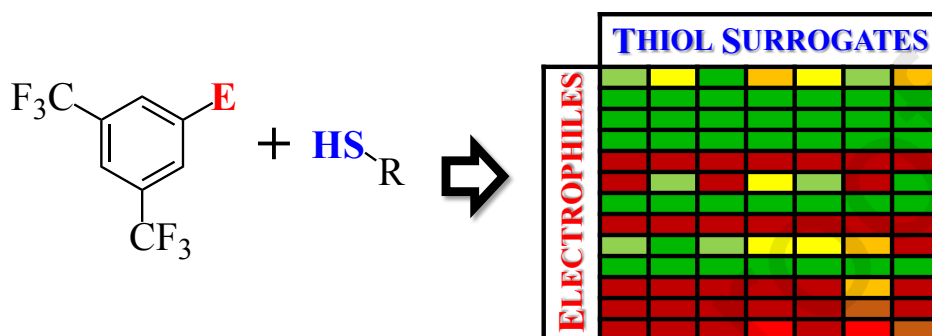
### References and notes

- Bauer RA. Covalent inhibitors in drug discovery: from accidental discoveries to avoided liabilities and designed therapies. *Drug Discov Today*. 2015;20(9):1061-1073. doi:10.1016/j.drudis.2015.05.005
- De Cesco S, Kurian J, Dufresne C, Mittermaier AK, Moitessier N. Covalent inhibitors design and discovery. *Eur J Med Chem*. 2017;138:96-114. doi:10.1016/j.ejmech.2017.06.019
- Singh J, Petter RC, Baillie TA, Whitty A. The resurgence of covalent drugs. *Nat Rev Drug Discov*. 2011;10(4):307-317. doi:10.1038/nrd3410
- González-Bello C. Designing Irreversible Inhibitors-Worth the Effort? *ChemMedChem*. 2016;11(1):22-30. doi:10.1002/cmdc.201500469
- Smith AJT, Zhang X, Leach AG, Houk KN. Beyond Picomolar Affinities: Quantitative Aspects of Noncovalent and Covalent

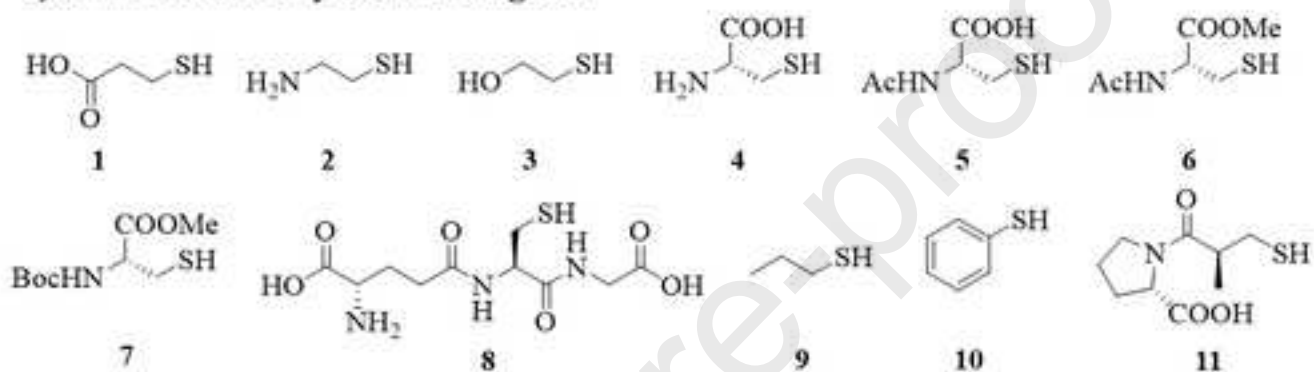
- doi:10.1021/jm800478c
6. Wei N, Li J, Fang C, et al. Targeting colon cancer with the novel STAT3 inhibitor bruceantinol. *Oncogene*. 2019;38(10):1676-1687. doi:10.1038/s41388-018-0547-y
  7. Kumaraswamy AA, Lewis AM, Geletu M, et al. Nanomolar-Potency Small Molecule Inhibitor of STAT5 Protein. *ACS Med Chem Lett*. 2014;5(11):1202-1206. doi:10.1021/ml500165r
  8. Wingelhofer B, Maurer B, Heyes EC, et al. Pharmacologic inhibition of STAT5 in acute myeloid leukemia. *Leukemia*. 2018;32(5):1135-1146. doi:10.1038/s41375-017-0005-9
  9. Tuley A, Fast W. The Taxonomy of Covalent Inhibitors. *Biochemistry*. 2018;57(24):3326-3337. doi:10.1021/acs.biochem.8b00315
  10. Shannon DA, Weerapana E. Covalent protein modification: the current landscape of residue-specific electrophiles. *Curr Opin Chem Biol*. 2015;24:18-26. doi:10.1016/j.cbpa.2014.10.021
  11. Embaby AM, Schoffelen S, Kofoed C, Meldal M, Diness F. Rational Tuning of Fluorobenzene Probes for Cysteine-Selective Protein Modification. *Angew Chemie Int Ed*. 2018;57(27):8022-8026. doi:10.1002/anie.201712589
  12. Gehringer M, Laufer SA. Emerging and Re-Emerging Warheads for Targeted Covalent Inhibitors: Applications in Medicinal Chemistry and Chemical Biology. *J Med Chem*. 2019;62(12):5673-5724. doi:10.1021/acs.jmedchem.8b01153
  13. Martín-Gago P, Olsen CA. Arylfluorosulfate-Based Electrophiles for Covalent Protein Labeling: A New Addition to the Arsenal. *Angew Chemie Int Ed*. 2019;58(4):957-966. doi:10.1002/anie.201806037
  14. Shindo N, Fuchida H, Sato M, et al. Selective and reversible modification of kinase cysteines with chlorofluoroacetamides. *Nat Chem Biol*. 2019;15(3):250-258. doi:10.1038/s41589-018-0204-3
  15. Weerapana E, Wang C, Simon GM, et al. Quantitative reactivity profiling predicts functional cysteines in proteomes. *Nature*. 2010;468(7325):790-795. doi:10.1038/nature09472
  16. Schwöbel JAH, Koleva YK, Enoch SJ, et al. Measurement and Estimation of Electrophilic Reactivity for Predictive Toxicology. *Chem Rev*. 2011;111(4):2562-2596. doi:10.1021/cr100098n
  17. Ábrányi-Balogh P, Petri L, Imre T, et al. A road map for prioritizing warheads for cysteine targeting covalent inhibitors. *Eur J Med Chem*. 2018;160:94-107. doi:10.1016/j.ejmech.2018.10.010
  18. Böhme A, Thaens D, Paschke A, Schüttmann G. Kinetic Glutathione Chemoassay To Quantify Thiol Reactivity of Organic Electrophiles □ Application to  $\alpha,\beta$ -Unsaturated Ketones, Acrylates, and Propiolates. *Chem Res Toxicol*. 2009;22(4):742-750. doi:10.1021/tx800492x
  19. Cee VJ, Volak LP, Chen Y, et al. Systematic Study of the Glutathione (GSH) Reactivity of N-Arylacrylamides: 1. Effects of Aryl Substitution. *J Med Chem*. 2015;58(23):9171-9178. doi:10.1021/acs.jmedchem.5b01018
  20. Flanagan ME, Abramite JA, Anderson DP, et al. Chemical and Computational Methods for the Characterization of Covalent Reactive Groups for the Prospective Design of Irreversible Inhibitors. *J Med Chem*. 2014;57(23):10072-10079. doi:10.1021/jm501412a
  21. Kathman SG, Statsyuk A V. Covalent tethering of fragments for covalent probe discovery. *Medchemcomm*. 2016;7(4):576-585. doi:10.1039/C5MD00518C
  22. Keeley A, Ábrányi-Balogh P, Keserü GM. Design and characterization of a heterocyclic electrophilic fragment library for the discovery of cysteine-targeted covalent inhibitors. *Medchemcomm*. 2019;10(2):263-267. doi:10.1039/C8MD00327K
  23. Martin JS, MacKenzie CJ, Fletcher D, Gilbert IH. Characterising covalent warhead reactivity. *Bioorg Med Chem*. 2019;27(10):2066-2074. doi:10.1016/j.bmc.2019.04.002
  24. Friedman M, Cavins JF, Wall JS. Relative Nucleophilic Reactivities of Amino Groups and Mercaptide Ions in Addition Reactions with  $\alpha,\beta$ -Unsaturated Compounds 1,2. *J Am Chem Soc*. 1965;87(16):3672-3682. doi:10.1021/ja01094a025
  25. Amslinger S, Al-Rifai N, Winter K, et al. Reactivity assessment of chalcones by a kinetic thiol assay. *Org Biomol Chem*. 2013;11(4):549-554. doi:10.1039/C2OB27163J
  26. Krishnan S, Miller RM, Tian B, Mullins RD, Jacobson MP, Taunton J. Design of Reversible, Cysteine-Targeted Michael Acceptors Guided by Kinetic and Computational Analysis. *J Am Chem Soc*. 2014;136(36):12624-12630. doi:10.1021/ja505194w
  27. Bent G-A, Maragh P, Dasgupta T. In vitro studies on the reaction rates of acrylamide with the key body-fluid thiols L-cysteine, glutathione, and captopril. *Toxicol Res*. 2014;3(6):445-446. doi:10.1021/acs.est.8b01675
  28. Dong S, Page MA, Wagner LD, Howa MB. Thiol Reactivity Analyses To Predict Mammalian Cell Cytotoxicity of Water Samples. *Environ Sci Technol*. 2018;52(15):8822-8829. doi:10.1021/acs.est.8b01675
  29. Kathman SG, Xu Z, Statsyuk A V. A Fragment-Based Method to Discover Irreversible Covalent Inhibitors of Cysteine Proteases. *J Med Chem*. 2014;57(11):4969-4974. doi:10.1021/jm500345q
  30. Alvarez-Sánchez R, Basketter D, Pease C, Lepoittevin J-P. Covalent binding of the <sup>13</sup>C-labeled skin sensitizers 5-chloro-2-methylisothiazol-3-one (MCI) and 2-methylisothiazol-3-one (MI) to a model peptide and glutathione. *Bioorg Med Chem Lett*. 2004;14(2):365-368. doi:10.1016/j.bmcl.2003.11.002
  31. MORRIS SJ, THURSTON DE, NEVELL TG. Evaluation of the electrophilicity of DNA-binding pyrrolo(2,1-c)(1,4)benzodiazepines by HPLC. *J Antibiot (Tokyo)*. 1990;43(10):1286-1292. doi:10.7164/antibiotics.43.1286
  32. Mackworth JF. The inhibition of thiol enzymes by lachrymators\*. *Biochem J*. 1948;42(1):82-90. doi:10.1042/bj0420082
  33. Saunders BC. Glutathione. Its reaction with alkali and some N and S derivatives. *Biochem J*. 1934;28(6):1977-1981. doi:10.1042/bj0281977
  34. Goddard DR, Schubert MP. The action of iodoethyl alcohol on thiol compounds and on proteins. *Biochem J*. 1935;29(5):1009-1011. doi:10.1042/bj0291009
  35. Hideji T, Kazuo H. Structure-toxicity relationship of acrylates and methacrylates. *Toxicol Lett*. 1982;11(1-2):125-129. doi:10.1016/0378-4274(82)90116-3
  36. MCCARTHY TJ, HAYES EP, SCHWARTZ CS, WITZ G. The Reactivity of Selected Acrylate Esters toward Glutathione and Deoxyribonucleosides in Vitro: Structure-Activity Relationships. *Toxicol Sci*. 1994;22(4):543-548. doi:10.1093/toxsci/22.4.543
  37. Fuller N, Spadola L, Cowen S, et al. An improved model for fragment-based lead generation at AstraZeneca. *Drug Discov Today*. 2016;21(8):1272-1283. doi:10.1016/j.drudis.2016.04.023
  38. Cravatt BF. Compositions and methods of modulating immune response. *WO2017210600/A1*. 2017.
  39. Al-Riyami L, Pineda MA, Rzepecka J, et al. Designing anti-inflammatory drugs from parasitic worms: A synthetic small molecule analogue of the acanthocheilonema viteae product ES-62 prevents development of collagen-induced arthritis. *J Med Chem*. 2013. doi:10.1021/jm401251p
  40. Callahan R, Ramirez O, Rosmarion K, Rothchild R, Bynum KC. Multinuclear NMR studies and ab initio structure calculations of hindered phencyclone diels-alder adducts from symmetrical cyclic dienophiles: Cyclohexene, vinylene carbonate, vinylene trithiocarbonate and two N-aryl maleimides. *J Heterocycl Chem*. 2005;42(5):889-898. doi:10.1002/jhet.5570420522
  41. Reddy TRK, Li C, Guo X, Fischer PM, Dekker L V. Design, synthesis and SAR exploration of tri-substituted 1,2,4-triazoles as inhibitors of the annexin A2-S100A10 protein interaction. *Bioorg Med Chem*. 2014;22(19):5378-5391. doi:10.1016/j.bmc.2014.07.043
  42. Chen Z-W, Ye D-N, Ye M, Zhou Z-G, Li S-H, Liu L-X. AgF/TFA-promoted highly efficient synthesis of  $\alpha$ -haloketones from haloalkynes. *Tetrahedron Lett*. 2014;55(7):1373-1375. doi:10.1016/j.tetlet.2014.01.027
  43. Weissman SA, Rossen K, Reider PJ. Stereoselective Synthesis of Styrene Oxides via a Mitsunobu Cyclodehydration. *Org Lett*. 2001;3(16):2513-2515. doi:10.1021/ol016167u
  44. Petersson MJ, Jenkins ID, Loughlin WA. The use of phosphonium anhydrides for the synthesis of 2-oxazolines, 2-thiazolines and 2-dihydrooxazine under mild conditions. *Org Biomol Chem*. 2009;7(4):739-746. doi:10.1039/B818310D

**Comparative reactivity analysis of small-molecule thiol surrogates**

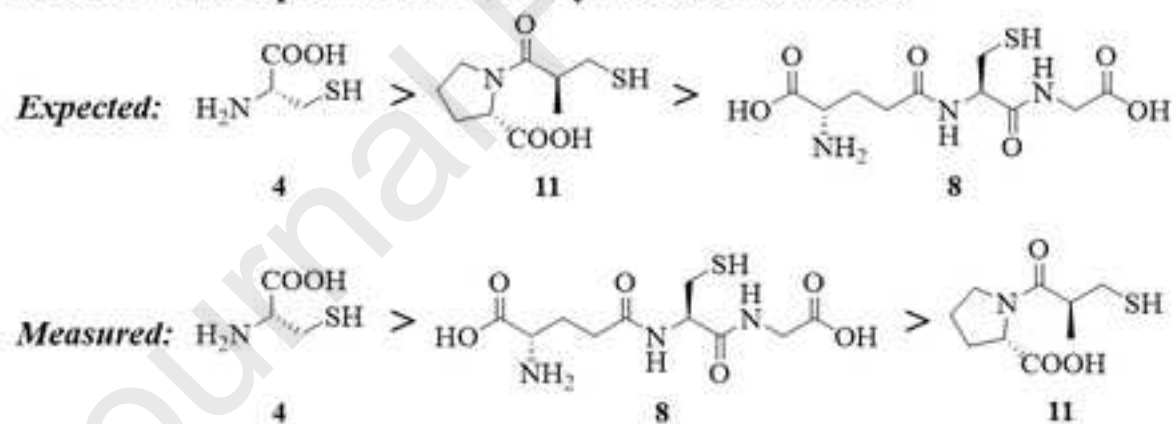
Leave this area blank for abstract info.

László Petri<sup>a</sup>, Péter Ábrányi-Balogh<sup>a</sup>, Petra Regina Varga<sup>a</sup>, Tímea Imre<sup>b</sup> and György Miklós Keserű<sup>a,\*</sup><sup>a</sup>Research Centre for Natural Sciences, Medicinal Chemistry Research Group, H-1117, Budapest, Magyar tudósok krt 2, HU.<sup>b</sup>Research Centre for Natural Sciences, MS Metabolomics Research Group, H-1117, Budapest, Magyar tudósok krt 2, HU.

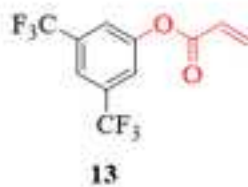
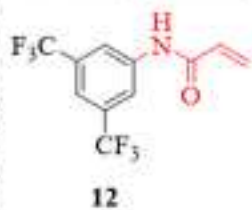
**a) Small molecule cysteine surrogates**



**b) Theoretical and experimental reactivity order of thiol models**



**Michael-type nucleophilic addition**



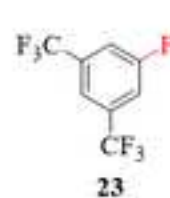
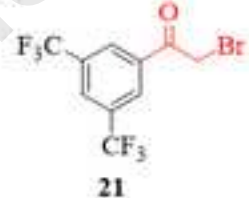
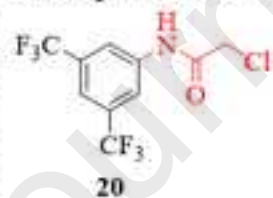
**Nucleophilic addition**

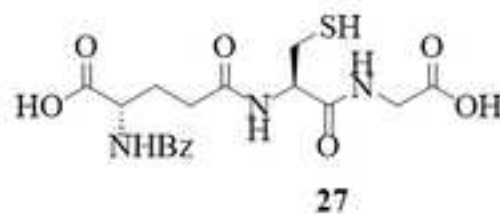
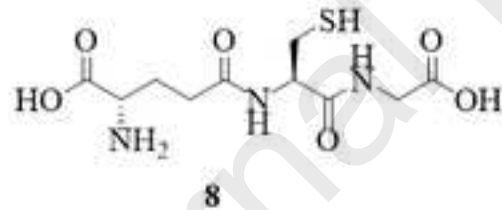
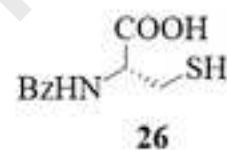
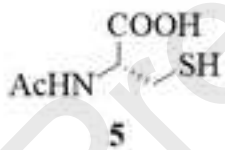
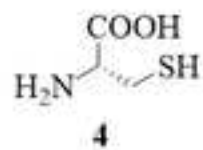
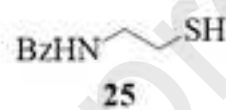
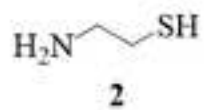


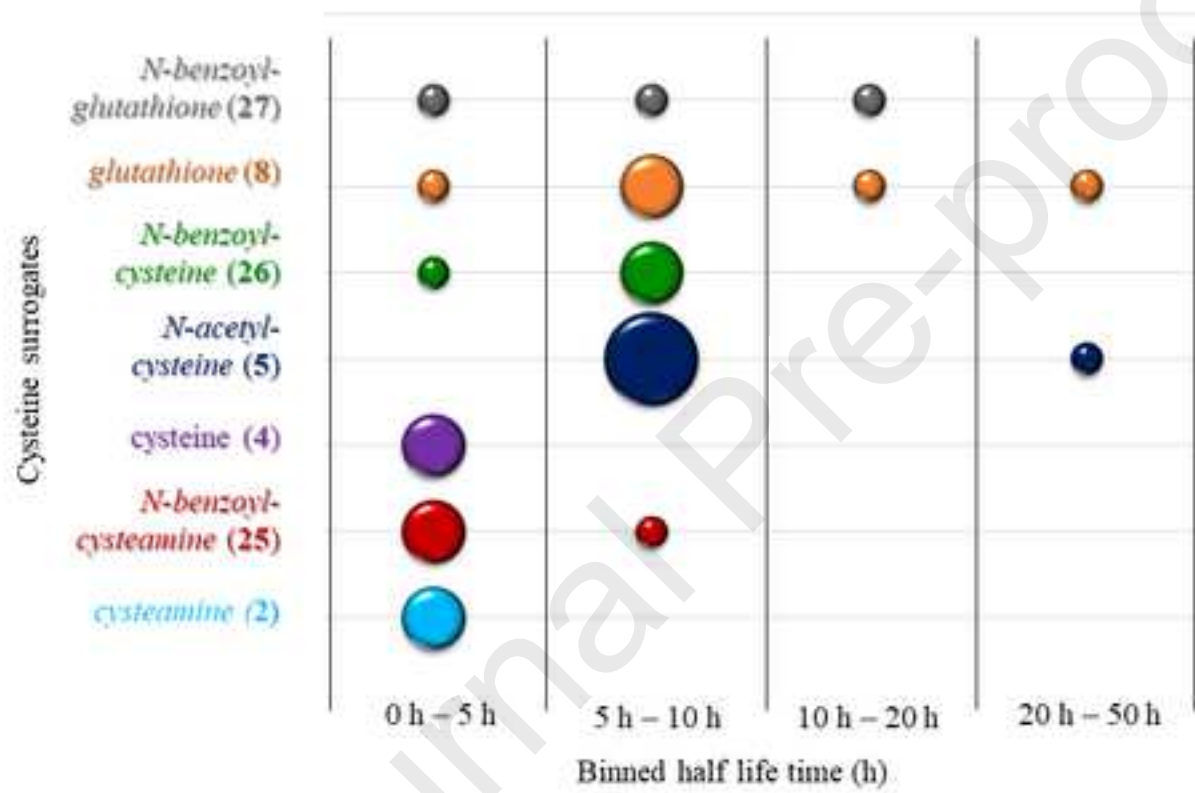
**Oxidation**



**Nucleophilic substitution**







Journal Pre-proofs

Entry	Warhead chemotype	cysteamine 2	<i>N</i> -benzoyl- cysteamine 25	cysteine 4	<i>N</i> -acetyl- cysteine 5	<i>N</i> -benzoyl- cysteine 26	glutathione 8	<i>N</i> -benzoyl- glutathione 27
12	acrylamide	1.8	5.3	0.8	6.1	5.5	4.2	5.7
13	acrylate	<0.017*	<0.017*	<0.017*	<0.017*	<0.017*	<0.017*	<0.017*
14	vinylsulfone	<0.017*	<0.017*	<0.017*	<0.017*	<0.017*	<0.017*	<0.017*
15	maleimide	<0.017*	<0.017*	<0.017*	<0.017*	<0.017*	<0.017*	<0.017*
16	styrene	>50	>50	>50	>50	>50	>50	>50
17	acetylene	>50	2.4	>50	5.9	1.6	>50	0.3
18	isothiocyanate	<0.017*	<0.017*	<0.017*	<0.017*	<0.017*	<0.017*	<0.017*
19	nitrile	>50	>50	>50	>50	>50	>50	>50
20	chloroacetamide	4.4	0.8	3.6	5.4	5.5	5.8	>50
21	bromoacetophenone	<0.017*	<0.017*	<0.017*	<0.017*	<0.017*	<0.017*	<0.017*
22	epoxide	>50	>50	>50	>50	>50	6.0	>50
23	fluorobenzene	>50	>50	>50	>50	>50	11.0	>50
24	thiol	>50	>50	>50	33.0	>50	31.5	11.2

The authors declare that they have no known competing financial interests or personal relationships that could have appeared to influence the work reported in this paper.

The authors declare the following financial interests/personal relationships which may be considered as potential competing interests: